

# Transcriptomic analyses of RNA-binding proteins reveal *eIF3c* promotes cell proliferation in hepatocellular carcinoma

Tangjian Li,<sup>1,3</sup> Shengli Li,<sup>1,3</sup> Di Chen,<sup>1</sup> Bing Chen,<sup>1</sup> Tao Yu,<sup>2</sup> Fangyu Zhao,<sup>2</sup> Qifeng Wang,<sup>1</sup> Ming Yao,<sup>2</sup> Shenglin Huang,<sup>1</sup> Zhiao Chen<sup>1</sup> and Xianghuo He<sup>1</sup> 

<sup>1</sup>Fudan University Shanghai Cancer Center and Institutes of Biomedical Sciences, Shanghai Medical College, Fudan University; <sup>2</sup>State Key Laboratory of Oncogenes and Related Genes, Shanghai Cancer Institute, Renji Hospital, Shanghai Jiao Tong University School of Medicine, Shanghai, China

## Key words

Cell proliferation, eukaryotic translation initiation factor 3 subunit C, hepatocellular carcinoma, RNA binding-proteins, the Cancer Genome Atlas

## Correspondence

Xianghuo He, Fudan University Shanghai Cancer Center and Institutes of Biomedical Sciences, Shanghai Medical College, Fudan University, Rm 1207, 2# Bldg, 270 Dong An Road, Shanghai 200032, China.

Tel: +86-21-34777577; Fax: +86-21-64172585;

E-mail: xhhe@fudan.edu.cn

and

Zhiao Chen, Fudan University Shanghai Cancer Center, Rm 1207, 2# Bldg, 270 Dong An Road, Shanghai 200032, China. Tel: +86-21-34777577; Fax: +86-21-64172585;

E-mail: zachen126@126.com

## Funding Information

National Natural Science Foundation of China; Shanghai Natural Science Fund.

<sup>3</sup>These authors contributed equally to this work.

Received October 31, 2016; Revised February 9, 2017; Accepted February 15, 2017

Cancer Sci 108 (2017) 877–885

doi: 10.1111/cas.13209

Primary liver cancer is the sixth most common cancer worldwide and is a leading cause of death in Asia.<sup>(1,2)</sup> Hepatocellular carcinoma is the most common form of liver cancer, and it is most often diagnosed during advanced stages of disease. The major risk factors for HCC include hepatitis B infection, hepatitis C infection, aflatoxin B exposure, alcohol consumption, and inherited metabolic diseases.<sup>(3)</sup> However, the molecular mechanisms underlying hepatic carcinogenesis remain elusive.

RNA-binding proteins often play multifunctional roles at every step of the RNA life cycle. RNA-binding proteins assemble into dynamic RNP (ribonucleoprotein) complexes that guide co- and post-transcriptional gene regulation, such as polyadenylation and alternative splicing, as well as RNA editing, transport, decay, stability, localization, and translation.<sup>(4–6)</sup> Dysregulated transcription of RBPs plays an important role in cancer development, as RBPs can impact the tumor formation and development through their interactions with microRNA,<sup>(7)</sup> mRNA,<sup>(8,9)</sup> long non-coding RNA,<sup>(10,11)</sup> and circular RNA.<sup>(12,13)</sup> Studies have examined the genome-

wide expression of RBPs in tumor and normal tissues<sup>(14–16)</sup> and have found that fluctuating RBP levels could result in tumorigenesis and correlate with patient prognosis. The Cancer Genome Atlas has generated comprehensive, multidimensional maps of key genomic changes in 33 types of cancer.<sup>(17–20)</sup> The Cancer Genome Atlas data consist of DNA methylation, gene expression, miRNA expression, exon expression, gene-level mutation, copy number, and clinical data for HCC patients; these data are publicly available and have been used frequently by the research community. The open-access nature of TCGA data provides a great resource to all researchers who seek to extend their knowledge in this area and to identify new methods for cancer treatment and prevention.

In this study, we referred to the latest RBP catalog, which includes 1542 genes,<sup>(21)</sup> approximately 7.5% of all human coding genes (<http://www.encodegenes.org>). By retrieving the transcriptional profiles of RBPs in the TCGA HCC dataset, we identified 92 RBP genes that displayed high expression in HCC tissue. Among the genes identified, 15 RBPs correlated with

poor patient prognosis. *eIF3c* was the gene most significantly associated with overall patient survival, and this gene was further shown to have an important role in hepatocarcinogenesis.

## Materials and Methods

**Cell lines and cell culture.** Huh-7, SK-HEP-1, and HEK-293T cells were obtained from the ATCC (Manassas, VA, USA). These cell lines were authenticated by ATCC based on morphology, karyotyping, and PCR assays. SMMC-7721 cells were obtained from Shanghai Second Military Medical University (Shanghai, China). All cells were cultured in a humidified 37°C incubator with a 5% CO<sub>2</sub> atmosphere in DMEM supplemented with 10% FBS, 100 U/mL penicillin, and 100 µg/mL streptomycin.

**Quantitative real-time PCR.** Total RNA was extracted using TRIzol reagent (Invitrogen, Carlsbad, CA, USA) according to the manufacturer's instructions. Complementary DNA was synthesized using the PrimeScriptRT reagent kit (TaKaRa, Tokyo, Japan). Real-time PCR analyses were carried out using SYBR Premix Ex Taq II (TaKaRa). The relative gene expression was calculated and normalized to β-actin using the comparative CT method. The primers that were used are listed in Table S1.

**Cell proliferation and colony formation assays.** Cell proliferation was measured with the CCK-8 (Dojindo, Kumamoto, Japan). Ten microliters of CCK-8 solution was added to each well once a day, and after 2 h of incubation at 37°C, the absorbance was measured at 450 nm. For colony formation assays, 1000 cells were seeded into each well of a six-well plate. Approximately 2 weeks after seeding, the cells were stained with 0.1% crystal violet and 20% methanol. Images were taken and the colonies were counted.

**Western blot analysis.** Proteins were separated by SDS-PAGE and transferred to nitrocellulose membranes (Bio-Rad, Hercules, CA, USA), after which the membranes were blocked in PBS/Tween-20 containing 5% non-fat milk. Then the membranes were probed with primary antibodies against eIF3c (Santa Cruz Biotechnology, Santa Cruz, CA, USA) overnight at 4°C. Immune-reactive bands were detected using SuperSignal West Femto Maximum Sensitivity Substrate (Thermo Fisher Scientific, Waltham, MA, USA).

**Lentivirus production and infection.** The ORF of *eIF3c* was amplified and cloned into the pWPXL lentiviral vector using a pEASY-Uni Seamless Cloning and Assembly kit (TransGen Biotech, Beijing, China). The construct was confirmed by DNA sequencing. Lentiviruses were generated by cotransfecting the lentiviral vector, the packaging plasmid psPAX2, and the VSV-G envelope plasmid pMD2.G (gifts from Dr Didier Trono, Laboratory of Virology and Genetics, Ecole Polytechnique Federale De Lausanne, Lausanne, Switzerland) into HEK-293T cells using Lipofectamine 2000 (Invitrogen). Supernatants were collected 48 h after transfection, filtered through a 0.45-µm membrane filter, and then used to infect HCC cells. Cells were infected with recombinant lentivirus plus 6 µg/mL polybrene (Sigma-Aldrich, St. Louis, MO, USA).

**Transfection of oligonucleotides.** The eIF3c siRNA duplexes were designed and synthesized by RiboBio (Guangzhou, China). For each well of a six-well plate, cells were transfected with a pool of three siRNAs in a total volume of 5 µL (20 µM) and 5 µL Lipofectamine 2000 (Invitrogen). Forty-eight hours after transfection, the cells were harvested for proliferation and colony formation assays. The three siRNA sequences are listed in Table S2.

**In vivo proliferation assays.** For the *in vivo* proliferation assays, SMMC-7721 cells stably expressing pWPXL-eIF3c or vector control were harvested and suspended in DMEM. Each

mouse (male BALB/c-nu/nu, 6 weeks old) was injected s.c. in the lower back with  $2 \times 10^6$  SMMC-7721 cells in 200 µL DMEM. After 6 weeks, mice were killed and examined for the growth of s.c. tumors. The mice were housed and manipulated using protocols approved by the Shanghai Medical Experimental Animal Care Commission.

**RNA preparation and sequencing.** Before constructing the RNA-seq libraries, 3 µg total RNA was processed using the RiboMinus Eukaryote kit (Qiagen, Valencia, CA, USA) to eliminate rRNA. Strand-specific RNA-seq libraries were prepared using the NEBNext Ultra Directional RNA Library Prep kit for Illumina (New England Biolabs, Beverly, MA, USA) according to the manufacturer's instructions. Briefly, ribosome-depleted RNA samples were first fragmented and then used for first- and second-strand cDNA synthesis with random hexamer primers. A dUTP mix was used for second-strand cDNA synthesis, which allows for the removal of the second strand. The cDNA fragments were treated with an End-It DNA End Repair kit to repair the ends, modified with the Klenow fragment to add an A at the 3'-end of the DNA fragments, and finally ligated with adaptor sequences. The ligated cDNA products were purified and treated with uracil DNA glycosylase to remove the second-strand cDNA. The libraries were subjected to quality control using a Bioanalyzer 2100 (Agilent, Santa Clara, CA, USA) and were sequenced using a HiSeq 3000 (Illumina, San Diego, CA, USA).

**Gene expression analysis of LIHC samples from TCGA.** RNA sequencing V2 read counts and patient clinical parameters based on 310 patients from the TCGA LIHC cohort were downloaded from the TCGA data portal (<https://tcga-data.nci.nih.gov/tcga/>), including 50 paired tumor/normal samples. Differential expression analysis was carried out using DESeq2<sup>(22)</sup> on the 50 paired samples. Genes that showed significantly differential expression (Benjamini–Hochberg corrected *P*-value  $\leq 0.05$  and log<sub>2</sub> fold-change  $\geq |1|$ ) between paired tumor and normal samples were selected for downstream analysis. Human RBPs cataloged by Gerstberger *et al.*,<sup>(21)</sup> which consists of 1542 RBPs, were used to identify all differentially expressed RBPs in the tumors. Gene-level somatic mutation data of the TCGA LIHC cohort were downloaded from the TCGA data portal (<https://tcga-data.nci.nih.gov/tcga/>).

**Survival and hazard analysis.** Expression levels across all tumor samples of each selected RBP gene were used to investigate whether the variation in the expression level of a given RBP gene is associated with prognosis in cancer patients. All tumor samples were dichotomized into two groups using the median expression level for each gene. The Kaplan–Meier method was further used to evaluate the overall survival time for the two groups. The differences of the survival times were compared using the log–rank test. All tests with a *P*-value less than 0.05 were considered significant. The Cox multivariate proportional hazards regression model was used to determine the independent factors that influence survival and recurrence based on the investigated variables.

**Gene Set Enrichment Analysis.** A GSEA<sup>(23)</sup> was used to identify genes (grouped as gene sets) comparatively enriched between Lenti-eIF3c overexpression and Lenti-NC control cells. Curated gene sets compiled from the Hallmark Gene Set Collection and the Kyoto Encyclopedia of Genes and Genomes were pulled from the GSEA's Molecular Signature Database. The expression data of overexpression and control cells were analyzed using the GSEA tool (version 2.2.1; Broad Institute, <http://www.broadinstitute.org/gsea/index.jsp>).

**Gene Ontology analysis.** Gene Ontology analysis was used to identify predominant biological processes of the differentially

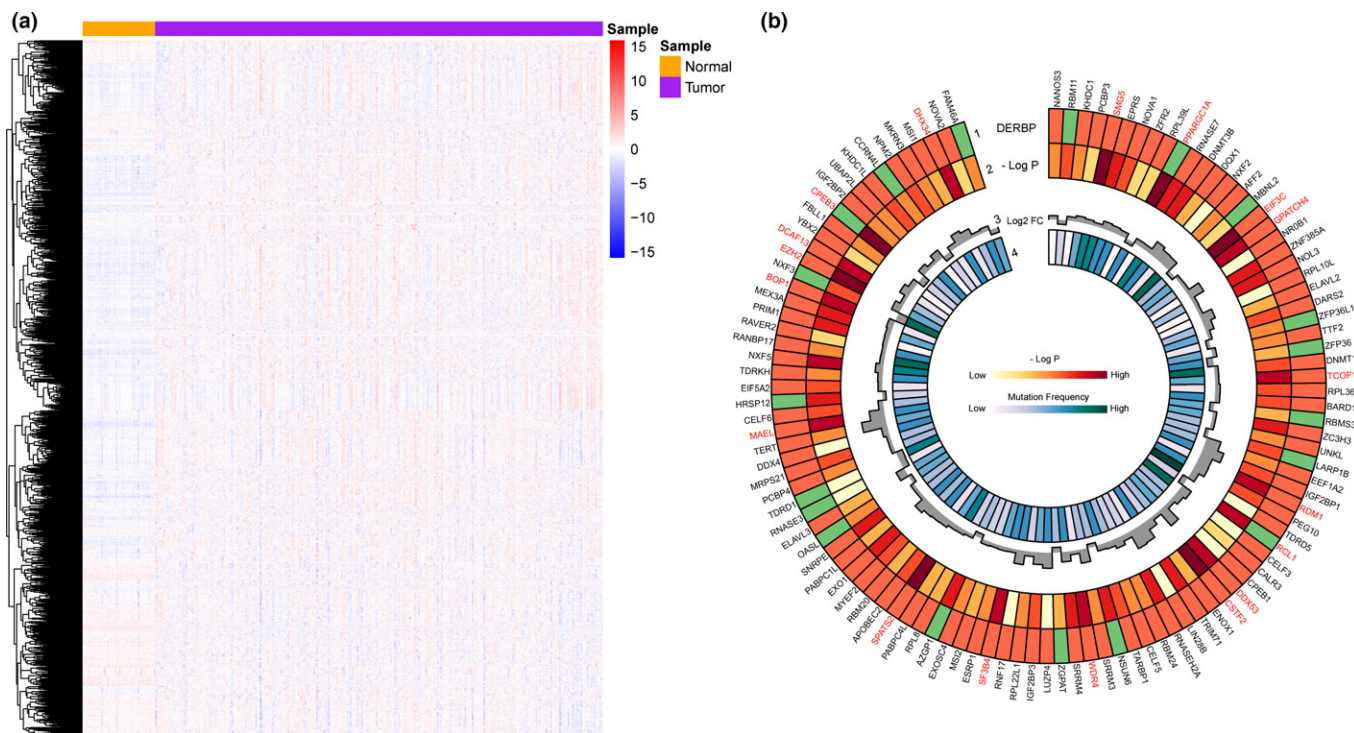


**Fig. 1.** Transcriptomic analyses of differentially expressed RNA-binding protein genes in The Cancer Genome Atlas. (a) Clustering heatmap for gene expression of 310 tumor samples and 50 normal samples from The Cancer Genome Atlas liver hepatocellular carcinoma cohort, with rows representing genes and columns representing samples. (b) Track 1 shows 92 upregulated (red boxes) and 19 downregulated (green boxes) RNA-binding protein genes in liver hepatocellular carcinoma samples. *P*-values on track 2 were generated from the survival analysis. Track 3 shows the fold-change of differentially expressed genes, and track 4 shows somatic mutation frequency. Genes whose expression levels were significantly associated with overall patient survival are shown in red.

expressed RBPs (92 upregulated and 19 downregulated genes). This analysis was done by the Bioconductor package “clusterProfiler”.<sup>(24)</sup>

**Statistical analysis.** Data are presented as mean  $\pm$  SEM from at least three independent experiments. A paired Student’s *t*-test was used to analyze differences in eIF3c mRNA expression levels among tumors and paired normal tissues in R software.<sup>(25)</sup> Survival analyses were carried out using the Kaplan–Meier method. Univariate and multivariate cox regression analyses were used to determine the independent factors that influence survival based on the investigated variables by using the SPSS Statistics version 22 package (IBM, Armonk, NY, USA). Differences in colony formation assay results between groups were analyzed using an unpaired Student’s *t*-test in GraphPad Prism 5 (<http://www.graphpad.com/>). Two-way ANOVA was used to analyze differences in the CCK-8 results between groups in GraphPad Prism 5. Plots were built using R software and GraphPad Prism 5, Circos.<sup>(26)</sup> A *P*-value  $<0.05$  was considered statistically significant.

## Results

**RNA-binding protein genes differentially expressed in LIHC samples.** To identify RBP genes that play a role in liver cancer development, we examined the expression profiles of 1542 RBP genes from TCGA dataset. Level-3 gene expression data and clinical parameters of 310 LIHC samples were retrieved from TCGA database (see Materials and Methods). To get a general understanding of the expression of all RBP genes in all samples, we used hierarchical agglomerative (complete

linkage) and Euclidean distance to undertake the hierarchical clustering (Fig. 1a). Paired tumor and normal samples (50 pairs) were used for the differential expression analysis. It was revealed that 92 human RBPs were upregulated in tumor samples compared with normal samples, whereas 19 RBP genes were downregulated (Fig. 1b, Table S3). Furthermore, we analyzed the differentially expressed RBPs (92 upregulated and 19 downregulated genes) through Gene Ontology analysis. The results showed that these differentially expressed RBP genes were correlated with RNA process, especially functions associated with RNA binding proteins, such as translation, RNA splicing, and mRNA transport (Fig. S1).

To determine whether these RBP genes are associated with poor prognosis in HCC, a survival analysis was carried out on all tumor samples to investigate the association of these differentially expressed RBP genes with overall survival. Clinical and expression data of 310 tumor samples were used for the survival analyses. For each RBP gene, tumor samples were classified into two groups according to median gene expression levels, and the differences in overall survival between these two groups were assessed. As a result, 15 upregulated and three downregulated RBP genes were significantly associated with overall survival ( $P < 0.05$ , log-rank test) (Fig. 1b). The somatic mutation frequencies of all the significantly differentially expressed genes in TCGA are also shown in Figure 1(b).

**High expression of eIF3c significantly correlates with cancer progression and poor prognosis in HCC patients.** To clearly show the significance on overall survival of the 15 upregulated and three downregulated RBP genes, we constructed survival

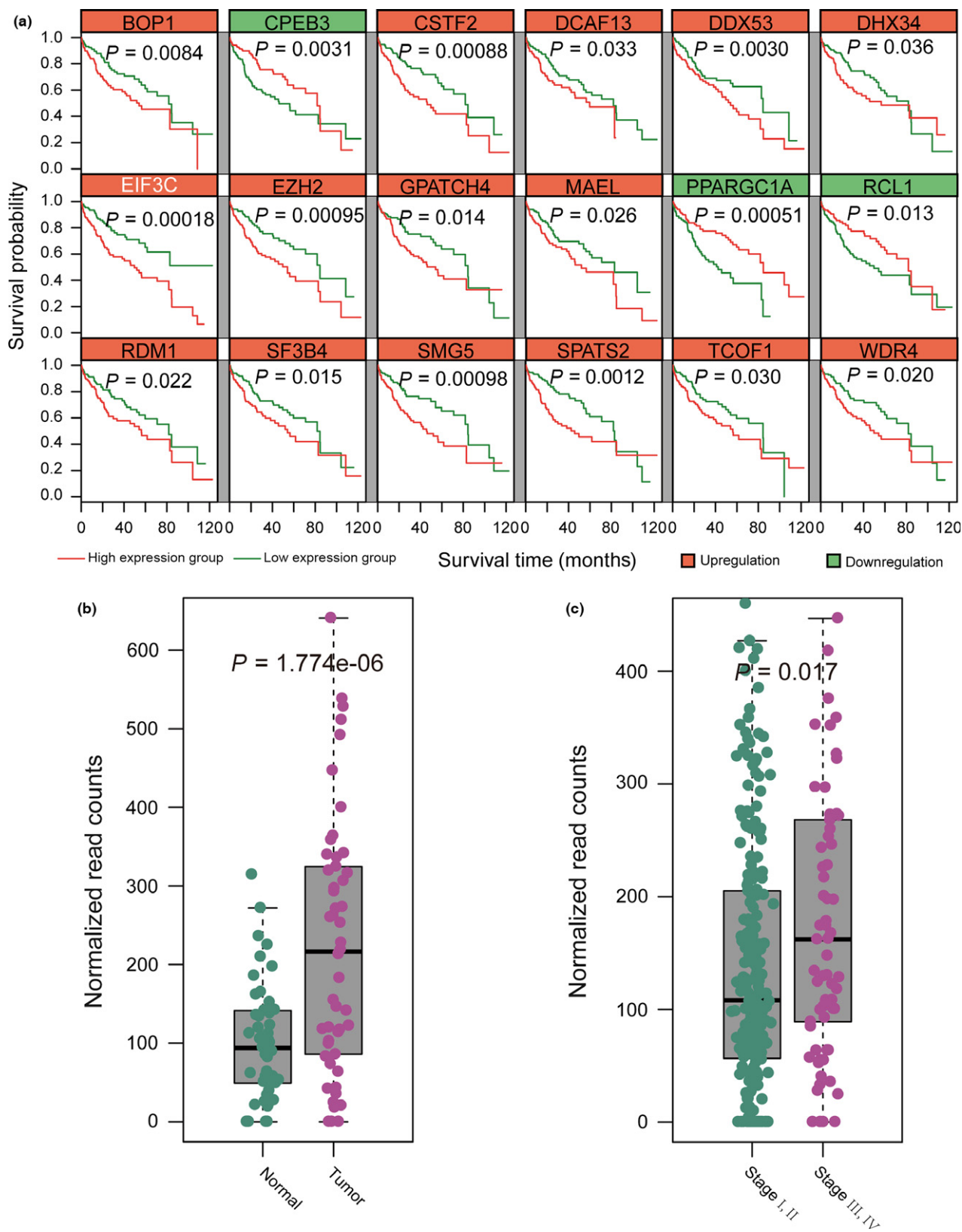


**Fig. 2.** Differential *eIF3c* expression implicates prognostic significance in liver hepatocellular carcinoma (LIHC) samples. (a) Survival curves of 15 upregulated RNA-binding protein (RBP) genes (red boxes) and three downregulated RBP genes (green boxes). Kaplan–Meier analysis of the correlation between RBP gene expression and overall patient survival. For each gene, patients were dichotomized into high expression (red lines) and low expression (green lines) groups using the median expression level of the individual genes. Log-rank tests were used to determine statistical significance. (b) *eIF3c* showed significantly higher expression ( $P = 1.774 \times 10^{-6}$ , paired Student’s *t*-test,) in the tumor samples relative to the paired normal samples from The Cancer Genome Atlas LIHC cohort. (c) *eIF3c* showed significantly higher expression ( $P = 0.017$ , unpaired Student’s *t*-test) in the poorly differentiated tumor samples from The Cancer Genome Atlas LIHC cohort.

**Table 1. Correlation of clinicopathological features with tumor *eIF3c* expression in The Cancer Genome Atlas liver hepatocellular carcinoma liver database**

Characteristic	Low <i>eIF3c</i> <i>n</i>	High <i>eIF3c</i> <i>n</i>	<i>P</i> -value	Total	Unknown
Age, years					
<60	73	63	0.252	310	0
≥60	82	92			
Gender					
Male	118	91	0.001	310	0
Female	37	64			
AFP, ng/mL					
<20	77	59	0.294	252	58
≥20	58	58			
Tumor differentiation					
I/II	128	113	0.041	310	0
III/IV	27	42			
Vascular invasion					
No	97	83	0.268	278	32
Micro/macro	46	52			

AFP,  $\alpha$ -fetoprotein.**Table 2. Univariate and multivariate analysis of factors associated with overall survival of patients with hepatocellular carcinoma with high *eIF3c* expression in The Cancer Genome Atlas liver hepatocellular carcinoma cohort**

Clinical variable	Hazard ratio	95% CI	<i>P</i> -value
Univariate analysis			
Age, years (≥60 vs <60)	1.414	0.932–2.144	0.104
Gender (female vs male)	1.398	0.929–2.105	0.108
AFP, ng/mL (≥20 vs <20)	1.448	0.908–2.310	0.120
Tumor differentiation (III/IV vs I/II)	1.965	1.287–3.001	0.002
Vascular invasion	1.354	0.860–2.132	0.191
<i>eIF3c</i> (high vs low)	2.19	1.436–3.339	0.000
Multivariate analysis			
Tumor differentiation (III/IV vs I/II)	1.848	1.208–2.828	0.005
<i>eIF3c</i> (high vs low)	2.101	1.337–3.208	0.001

CI, confidence interval.

curves for these RBPs. As expected, the survival time was significantly different between patients in the two expression groups, and low *eIF3c* expression correlated with better prognosis. Among these survival-associated RBP genes, *eIF3c* showed the highest prognostic contribution of candidate RBPs by calculating the hazard ratio (2.19;  $P < 0.001$ , Cox regression analyses) (Fig. 2a, Table S4). Moreover, *eIF3c* expression was significantly higher in tumor samples compared with paired normal samples from the TCGA LIHC cohort (Fig. 2b). Additionally, we investigated a possible correlation between clinicopathological features and tumor *eIF3c* expression in TCGA LIHC patients. Our analysis revealed that poorly differentiated tumors show significant correlation with high *eIF3c* expression levels (Fig. 2c, Table 1).

To investigate whether the expression levels of *eIF3c* were independent of other predictive variables, we applied multivariate analyses using a Cox multivariate proportional hazard

regression model comparing *eIF3c* expression and clinicopathological factors (age, gender, tumor size, vascular invasion, and stage) as covariates. The univariate analysis showed that TNM stage and the expression of *eIF3c* were factors that were consistently significantly associated with overall survival in TCGA cohorts. In addition, a multivariate statistical analysis revealed that HCC patients with high tumor *eIF3c* expression harbored a 2.101-fold higher risk of death (95% confidence interval, 1.208–2.828,  $P = 0.001$ ) (Table 2). Thus, the above analysis showed that upregulated expression of *eIF3c* is an independent unfavorable prognostic factor in HCC.

***eIF3c* promotes HCC cell proliferation *in vitro* and tumor growth *in vivo*.** To determine the functional roles of *eIF3c* in HCC, we first knocked down the expression of the *eIF3c* gene in SMMC-7721 and SK-HEP-1 cells. The knockdown efficiency was validated by quantitative real-time PCR and immunoblotting (Fig. S2). Subsequently, the effect of *eIF3c* knockdown on proliferation was determined by CCK-8 assays and colony formation assays (Fig. 3a,b). Our results showed that disruption of *eIF3c* gene expression significantly decreased the proliferation of SMMC-7721 and SK-HEP-1 cells.

Furthermore, we overexpressed the *eIF3c* gene in SMMC-7721 and Huh-7 cells using a lentivirus system to establish two stable *eIF3c*-overexpressing cell lines. The overexpression efficiency was determined by quantitative real-time PCR and immunoblotting (Fig. S3). Subsequently, the effect of *eIF3c* overexpression on proliferation was determined by CCK-8 assays and colony formation assays (Fig. 3c,d). The results showed that overexpression of the *eIF3c* gene significantly increased the proliferation of SMMC-7721 and Huh-7 cells. To further characterize the effects of *eIF3c* on HCC tumor growth *in vivo*, SMMC-7721 transduced with Lenti-*eIF3c* and Lenti-vector were s.c. implanted into the flanks of nude mice, and these mice were monitored closely for tumor growth for 6 weeks. Our results showed that tumors derived from Lenti-vector cells were significantly smaller than those derived from Lenti-*eIF3c* cells in terms of both tumor volumes and weights (Fig. 3e,f). The above results indicate that *eIF3c* significantly promotes HCC cell proliferation *in vitro* and *in vivo*.

**Gene Set Enrichment Analysis of *eIF3c*-associated signaling pathways.** To assess the contribution of *eIF3c* to HCC development, we enforced *eIF3c* overexpression in SMMC-7721 cells and then undertook RNA-seq analysis. We then mapped changes in transcriptomic profile events relative to control samples and found 347 upregulated genes and 195 downregulated genes ( $|\log_2 \text{fold-change}| > 1$ ) (Table S5). To gain further insight into the biological roles of *eIF3c* in HCC in an unbiased manner, we applied GSEA of the RNA-seq data and found that high *eIF3c* expression positively correlated with changes in the KRAS, VEGF, and Hedgehog signaling pathways, all of which were selected according to nominal *P*-value rank (Tables S6,S7), and were closely related with specific cancer-related gene sets (Fig. 4a–c). Next, we selected the upregulated genes ( $\log_2 \text{fold-change} > 1$ ) (Table S8) enriched in the aforementioned three pathways for validation. Real-time PCR analyses showed that alteration of *eIF3c* expression significantly increased the expression of most of the selected genes, including *WNT5B*, *DHH*, *SMO*, *RAC2*, *PCSKIN*, and *INMBA* (Fig. 4d). The oncogenic function of *RAC2* has been reported in HCC,<sup>(27)</sup> and *WNT5B*,<sup>(28)</sup> *SMO*,<sup>(29)</sup> *DHH*,<sup>(30)</sup> *PCSKIN*,<sup>(31)</sup> and *INHBA* have also been studied in other cancers.<sup>(32)</sup> These data suggest that *eIF3c* may activate specific

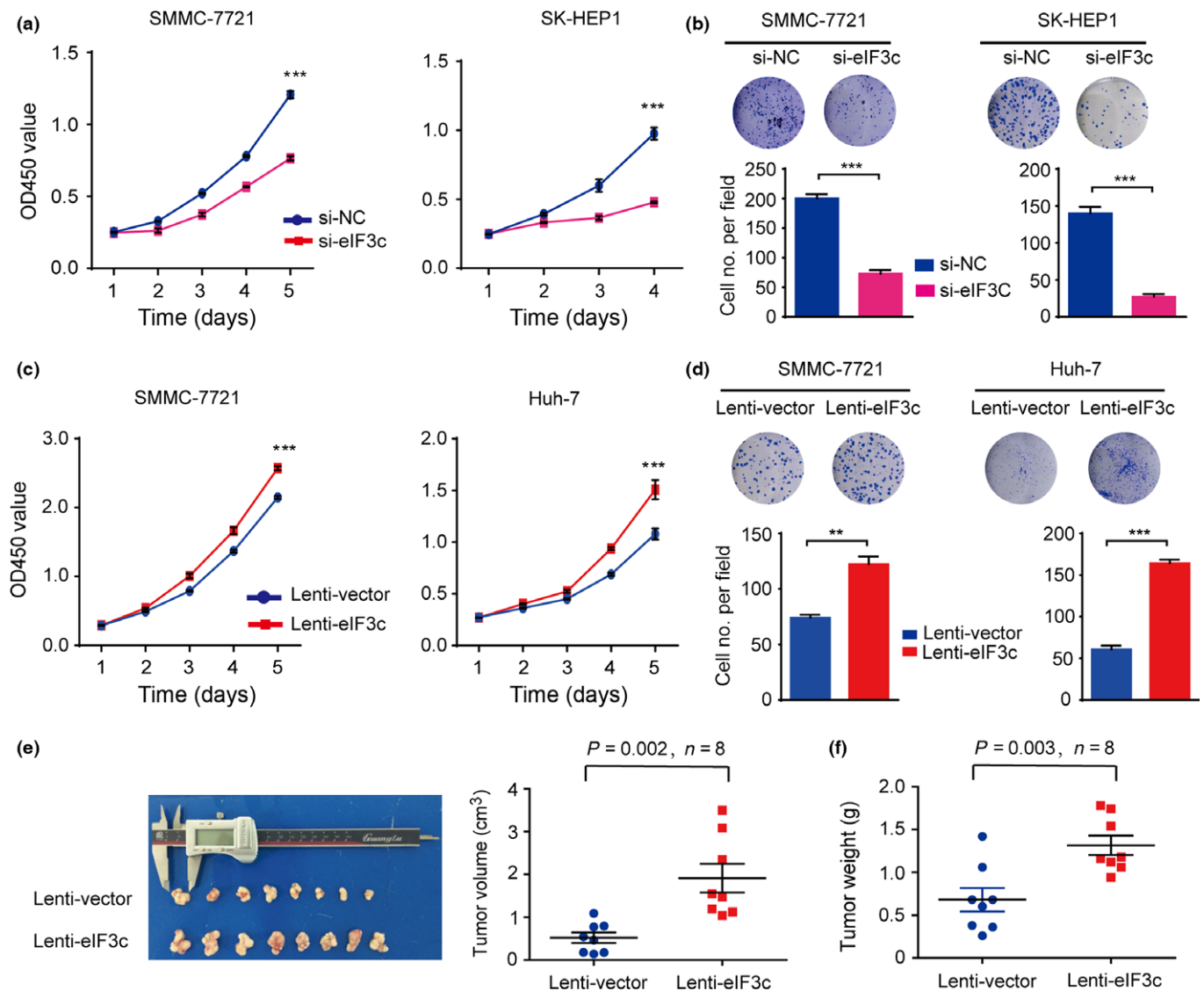


**Fig. 3.** eIF3c promotes hepatocellular carcinoma cell proliferation *in vitro* and tumor growth *in vivo*. (a) Proliferation of SMMC-7721 and SK-HEP-1 cells targeted by a pool of three eIF3c siRNAs was measured using a cell counting assay. (b) Colony formation for SMMC-7721 and SK-HEP-1 cells transfected with a pool of three eIF3c siRNAs was measured using a colony formation assay. (c) Proliferation of SMMC-7721 and Huh-7 cells overexpressing eIF3c was measured using a cell counting assay. (d) Colony formation results for SMMC-7721 and Huh-7 cells overexpressing eIF3c are shown. (e, f) Overexpression of eIF3c increased the volume and weight of xenograft tumors. \* $P < 0.05$ ; \*\* $P < 0.01$ ; \*\*\* $P < 0.001$ . ns, not significant.

oncogenic signaling pathways to promote liver cancer cell proliferation.

## Discussion

Given the central role of RBPs in the regulation of gene expression, it comes as no surprise that RBP malfunction can lead to disease, including cancer.<sup>(33–35)</sup> Major changes in RBP expression have been reported in numerous types of cancer.<sup>(14,15,36,37)</sup> In a previous study, Gutschner *et al.* reported a microarray analysis of 60 HCC and 7 normal liver samples to analyze RBPs induced in human liver cancer, and they found that the most strongly upregulated RBP was insulin-like growth factor 2 mRNA-binding protein one. This RBP was also shown to have a broad impact on HCC cell proliferation, survival, and tumor growth.<sup>(38)</sup> In the present study, we applied

a combination of transcriptomic analyses followed by a Kaplan–Meier analysis to evaluate the relationship of the expression of potentially oncogenic RBP genes with patient prognosis in 310 TCGA tumor samples. A total of 15 RBPs showed at least a two-fold change in gene expression and were associated with poor prognosis, suggesting their potential impact on tumor progression and aggressiveness.

The functions of most of the 15 upregulated RBP genes have been explored in disease, especially in cancer. For instance, the levels of *CSTF2* increase as cells enter S phase, and its depletion affects histone RNA processing, S phase progression, and cell proliferation.<sup>(39)</sup> *EZH2*, a histone methyltransferase subunit of the polycomb repressor complex, is often mutated in several types of cancer and is aberrantly overexpressed in many others.<sup>(40)</sup> Previous reports have suggested that *BOP1* plays an oncogenic role in HCC by inducing

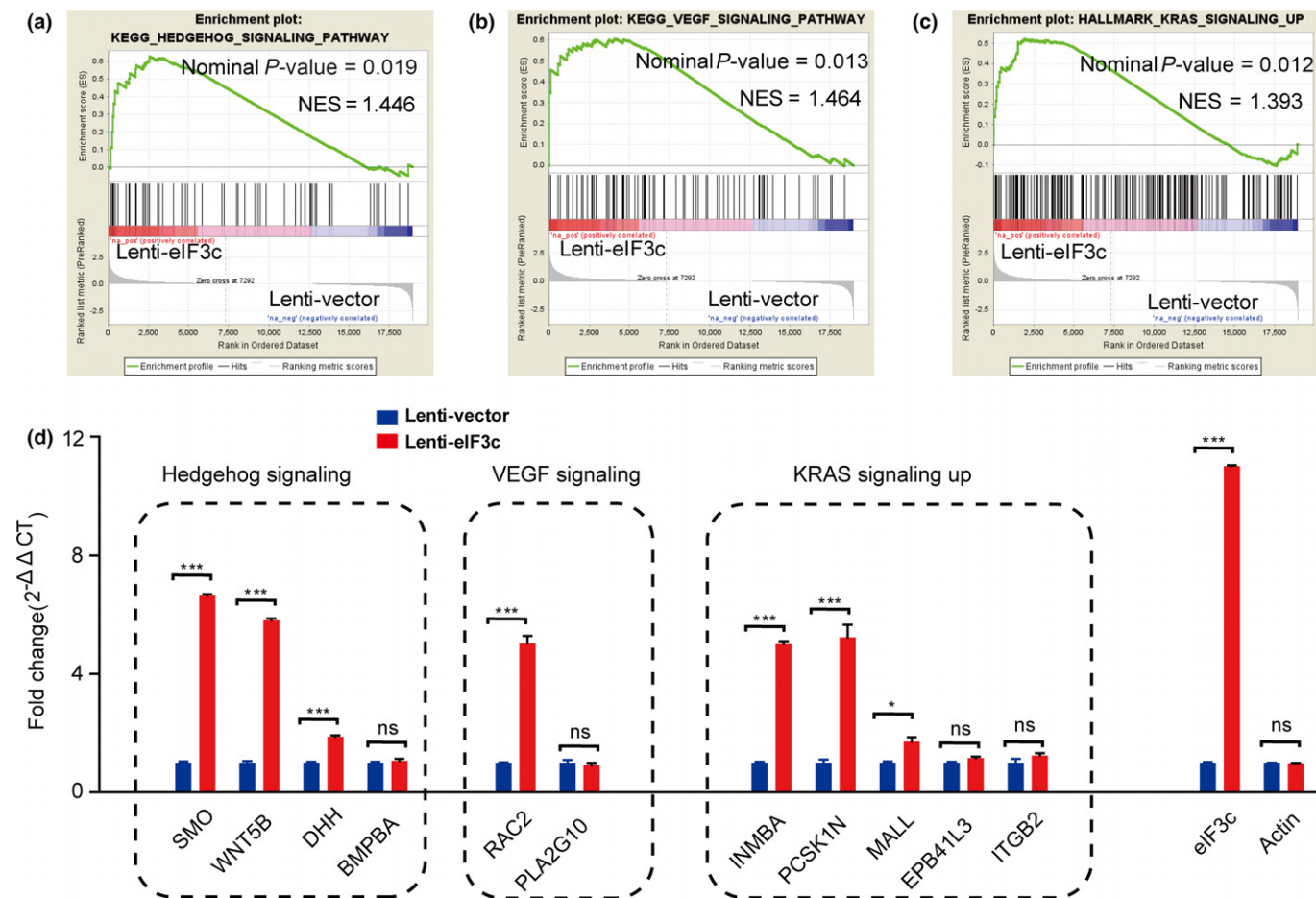


**Fig. 4.** Gene Set Enrichment Analysis of *eIF3c*-activated cancer-related pathways. (a–c) Genes in the hallmark Kyoto Encyclopedia of Genes and Genomes (KEGG) Hedgehog, KEGG vascular endothelial growth factor (VEGF), and KRAS signaling pathways showed significant enrichment in high-expression *eIF3c* versus normal-expression *eIF3c* in SMMC-7721 Lenti-*eIF3c* and Lenti-vector cell lines based on RNA sequencing. The top portion of each panel shows the normalized enrichment scores (NES) for each gene; the bottom portion of the plot indicates the value of the ranking metric moving down the list of ranked genes. (d) Real-time PCR analysis revealed a significant increase in the expression levels of *SMO*, *WNT5B*, *DHH*, *RAC2*, *PCSK1N*, and *INMBA* in SMMC-7721 cells infected with Lenti-*eIF3c*. \* $P < 0.05$ ; \*\* $P < 0.01$ ; \*\*\* $P < 0.001$ . ns, not significant.

epithelial–mesenchymal transition and promoting actin cytoskeleton remodeling.<sup>(41)</sup> A novel oncogene, *MAEL*, is frequently overexpressed in HCC and is significantly associated with HCC recurrence and poor outcome. Moreover, *MAEL* plays an important role in the development and progression of HCC by inducing epithelial–mesenchymal transition through the protein kinase B/glycogen synthase kinase-3 $\beta$ /Snail signaling pathway.<sup>(42)</sup>

As the largest initiation factor, *eIF3* plays vital roles in translation initiation. Some of the *eIF3* subunits have shown oncogenic roles in various cancers. Previous studies have shown that ectopic expression of *eIF3c* in stably transfected NIH3T3 cells increased clonogenicity and viability and facilitated S phase entry and attenuation of apoptosis.<sup>(43)</sup> *eIF3c* may promote seminoma development by generally increasing translation, leading to enhanced cellular growth and division rates.<sup>(44)</sup> Knockdown of *eIF3c* significantly decreased cell proliferation and colony formation and further induced cell cycle arrest and apoptosis in the RKO cell line.<sup>(45)</sup> Most importantly, Emmanuel *et al.* reported that *eIF3c* is vital to translation initiation *in vivo*, as its downregulation decreases global protein synthesis and causes a polysome run-off. Furthermore, they emphasized the importance of *eIF3c* as a therapeutic target for heterogeneous malignancies.<sup>(46)</sup> However, no causal relationship has

been established between *eIF3c* expression levels and HCC development. In the present study, we showed that the expression of *eIF3c* was significantly different in 50 paired TCGA samples, and high *eIF3c* expression correlated with poor patient prognosis in 310 tumor TCGA samples. Furthermore, multivariate analysis showed that the upregulated expression of *eIF3c* is an independent unfavorable prognostic factor in HCC. In addition, we confirmed the role of *eIF3c* in proliferation by using siRNA and lentivirus overexpression systems as well as *in vivo* experiments to further verify our *in vitro* results.

For a preliminary exploration of the *eIF3c* oncogenic mechanism, we developed SMMC-7721 Lenti-*eIF3c* and Lenti-vector cells and then undertook RNA-seq analysis. Gene Set Enrichment Analysis of the RNA-seq data showed that the KRAS, VEGF, and Hedgehog signaling pathways were differentially expressed. Aberrant activation of the KRAS, VEGF, and Hedgehog signaling pathways can drive tumorigenesis, in part through the promotion of cell growth. We further confirmed the upregulation of selected target genes, and these results suggest that *eIF3c* exerts its regulatory effects through these signaling pathways. Among the upregulated genes, *WNT5B* induces tube formation by regulating the expression of Snail and Slug proteins through the activation of canonical and non-canonical WNT signaling pathways in oral squamous cell

carcinoma.<sup>(28)</sup> The combined inhibition of *SMO* and *EGFR* exerts strong antiproliferative activity with complete inhibition of phosphatidylinositol 3-kinase/protein kinase B and MAPK phosphorylation.<sup>(29)</sup> *INHBA* could strongly induce embryonic stem cell differentiation.<sup>(47)</sup> Taken together, these results suggest that *eIF3c* might promote HCC cell proliferation through the activation of these signaling pathways. However, further investigation is required to elucidate the detailed mechanisms.

In conclusion, we showed that *eIF3c* regulates HCC cell proliferation *in vitro* and tumorigenesis *in vivo*. Increased *eIF3c* expression positively correlated with the activation of several oncogenic pathways. Despite the need for a more detailed analysis to determine how *eIF3c* exerts its growth-promoting function, our study provides a novel way to investigate the molecular mechanism by which *eIF3c* influences liver tumor progression.

### Acknowledgments

We are grateful for Dr T. Didier's gifts of the pWPXL, psPAX2, and pMD2.G lenti-virus plasmids. This work was supported by grants from

the National Natural Science Foundation of China (Grant No. 81201538) and Shanghai Natural Science Fund (Grant No. 12ZR1449900).

### Disclosure Statement

The authors have no conflict of interest.

### Abbreviations

CCK-8	Cell Counting Kit-8
eIF3c	eukaryotic translation initiation factor 3 subunit C
GSEA	gene set enrichment analysis
HCC	hepatocellular carcinoma
RBP	RNA-binding protein
RNA-seq	RNA sequencing
TCGA	The Cancer Genome Atlas
VEGF	vascular endothelial growth factor
SEM	standard error of the mean
LIHC	liver hepatocellular carcinoma

### References

- Stewart B, Wild C. *World Cancer Report 2014*. Lyon, Geneva: International Agency for Research on Cancer, 2014.
- Naghavi M, Wang H, Lozano R *et al*. Global, regional, and national age-sex specific all-cause and cause-specific mortality for 240 causes of death, 1990–2013: a systematic analysis for the Global Burden of Disease Study 2013. *Lancet* 2015; **385**: 117–71.
- El-Serag HB. Epidemiology of viral hepatitis and hepatocellular carcinoma. *Gastroenterology* 2012; **142**: 1264–73.e1.
- Zhang S, Zhou J, Hu H *et al*. A deep learning framework for modeling structural features of RNA-binding protein targets. *Nucleic Acids Res* 2016; **44**: e32.
- Ray D, Kazan H, Cook KB *et al*. A compendium of RNA-binding motifs for decoding gene regulation. *Nature* 2013; **499**: 172–7.
- Spitale RC, Flynn RA, Zhang QC *et al*. Structural imprints *in vivo* decode RNA regulatory mechanisms. *Nature* 2015; **519**: 486–90.
- Ciafre SA, Galardi S. microRNAs and RNA-binding proteins: a complex network of interactions and reciprocal regulations in cancer. *RNA Biol* 2013; **10**: 935–42.
- Grammatikakis I, Abdelmohsen K, Gorospe M. *Posttranslational Control of HuR Function*. Wiley interdisciplinary reviews RNA. 2017; 8.
- Frisone P, Pradella D, Di Matteo A, Belloni E, Ghigna C, Paronetto MP. Sam68: signal transduction and RNA metabolism in human cancer. *Biomed Res Int* 2015; **2015**: <http://dx.doi.org/10.1155/2015/528954>.
- Luo M, Li Z, Wang W, Zeng Y, Liu Z, Qiu J. Long non-coding RNA H19 increases bladder cancer metastasis by associating with EZH2 and inhibiting E-cadherin expression. *Cancer Lett* 2013; **333**: 213–21.
- Schmitt AM, Chang HY. Long noncoding RNAs in cancer pathways. *Cancer Cell* 2016; **29**: 452–63.
- Conn SJ, Pillman KA, Toubia J *et al*. The RNA binding protein quaking regulates formation of circRNAs. *Cell* 2015; **160**: 1125–34.
- Peng L, Yuan XQ, Li GC. The emerging landscape of circular RNA ciRS-7 in cancer (Review). *Oncol Rep* 2015; **33**: 2669–74.
- Kechavarzi B, Janga SC. Dissecting the expression landscape of RNA-binding proteins in human cancers. *Genome Biol* 2014; **15**: 1.
- Correa BR, de Araujo PR, Qiao M *et al*. Functional genomics analyses of RNA-binding proteins reveal the splicing regulator SNRNP as an oncogenic candidate in glioblastoma. *Genome Biol* 2016; **17**: 1.
- Beebe TW, Cieply BW, Carstens RP. Genome-Wide Activities of RNA Binding Proteins that Regulate Cellular Changes in the Epithelial to Mesenchymal Transition (EMT). *Adv Exp Med Biol* 2014; **825**: 267–302.
- Chin L, Andersen JN, Futreal PA. Cancer genomics: from discovery science to personalized medicine. *Nat Med* 2011; **17**: 297–303.
- Chin L, Hahn WC, Getz G, Meyerson M. Making sense of cancer genomic data. *Genes Dev* 2011; **25**: 534–55.
- Tomczak K, Czerwinska P, Wiznerowicz M. The Cancer Genome Atlas (TCGA): an immeasurable source of knowledge. *Contemp Oncol (Pozn)* 2015; **19**: A68–77.
- Koboldt D. The future of cancer genomics. *Clin OMICS* 2014; **1**: 8–10.
- Gerstberger S, Hafner M, Tuschl T. A census of human RNA-binding proteins. *Nat Rev Genet* 2014; **15**: 829.
- Love MI, Huber W, Anders S. Moderated estimation of fold change and dispersion for RNA-seq data with DESeq2. *Genome Biol* 2014; **15**: 1.
- Subramanian A, Tamayo P, Mootha VK *et al*. Gene set enrichment analysis: a knowledge-based approach for interpreting genome-wide expression profiles. *Proc Natl Acad Sci* 2005; **102**: 15545–50.
- Yu G, Wang LG, Han Y, He QY. clusterProfiler: an R package for comparing biological themes among gene clusters. *OMICS* 2012; **16**: 284–7.
- Team RC. *R: A Language and Environment for Statistical Computing*. 2013; **1**: 12–21.
- Krzywinski M, Schein J, Birol I *et al*. Circos: an information aesthetic for comparative genomics. *Genome Res* 2009; **19**: 1639–45.
- Zhang J-Y, Weng M-Z, Song F-B *et al*. Long noncoding RNA AFAP1-AS1 indicates a poor prognosis of hepatocellular carcinoma and promotes cell proliferation and invasion via upregulation of the RhoA/Rac2 signaling. *Int J Oncol* 2016; **48**: 1590–8.
- Wang S, Chang JS, Hsiao J *et al*. Tumour cell-derived WNT5B modulates *in vitro* lymphangiogenesis via induction of partial endothelial-mesenchymal transition of lymphatic endothelial cells. *Oncogene* 2017; **36**: 1503–15.
- Corte CMD, Bellevisine C, Vicidomini G *et al*. *SMO* gene amplification and activation of the Hedgehog pathway as novel mechanisms of resistance to anti-epidermal growth factor receptor drugs in human lung cancer. *Clin Cancer Res* 2015; **21**: 4686–97.
- Chinchilla P, Xiao L, Kazanietz MG, Riobo NA. Hedgehog proteins activate pro-angiogenic responses in endothelial cells through non-canonical signaling pathways. *Cell Cycle* 2010; **9**: 570–9.
- Bergamaschi A, Christensen BL, Katzenellenbogen BS. Reversal of endocrine resistance in breast cancer: interrelationships among 14-3-3 $\zeta$ , FOXM1, and a gene signature associated with mitosis. *Breast Cancer Res* 2011; **13**: 1.
- Wang Q, Wen Y-G, Li D-P *et al*. Upregulated *INHBA* expression is associated with poor survival in gastric cancer. *Med Oncol* 2012; **29**: 77–83.
- Castello A, Fischer B, Hentze MW, Preiss T. RNA-binding proteins in Mendelian disease. *Trends Genet* 2013; **29**: 318–27.
- Cooper TA, Wan L, Dreyfuss G. RNA and disease. *Cell* 2009; **136**: 777–93.
- Lukong KE, Chang K-w, Khandjian EW, Richard S. RNA-binding proteins in human genetic disease. *Trends Genet* 2008; **24**: 416–25.
- Galante PA, Sandhu D, de Sousa Abreu R *et al*. A comprehensive *in silico* expression analysis of RNA binding proteins in normal and tumor tissue; identification of potential players in tumor formation. *RNA Biol* 2009; **6**: 426–33.
- Wang J, Liu Q, Shyr Y. Dysregulated transcription across diverse cancer types reveals the importance of RNA-binding protein in carcinogenesis. *BMC Genom* 2015; **16**: 1.
- Gutschner T, Hammerle M, Pazaitis N *et al*. Insulinulin diverse cancer types reveals the importance of RNA-binding prant protumorigenic factor in hepatocellular carcinoma. *Hepatology* 2014; **59**: 1900–11.

- 39 Romeo V, Griesbach E, Schumperli D. CstF64: cell cycle regulation and functional role in 3' End processing of replication-dependent histone mRNAs. *Mol Cell Biol* 2014; **34**: 4272–84.
- 40 Kim KH, Roberts CW. Targeting EZH2 in cancer. *Nat Med* 2016; **22**: 128–34.
- 41 Chung K, Cheng IK, Ching AKK, Chu J, Lai PBS, Wong N. Block of proliferation 1 (BOP1) plays an oncogenic role in hepatocellular carcinoma by promoting epithelial-to-mesenchymal transition. *Hepatology* 2011; **54**: 307–18.
- 42 Liu L, Dai Y, Chen J et al. Maelstrom promotes hepatocellular carcinoma metastasis by inducing epithelial-mesenchymal transition by way of Akt/GSK-3 $\beta$ /Snail signaling. *Hepatology* 2014; **59**: 531–43.
- 43 Zhang L, Pan X, Hershey JWB. Individual overexpression of five subunits of human translation initiation factor eIF3 promotes malignant transformation of immortal fibroblast cells. *J Biol Chem* 2007; **282**: 5790–800.
- 44 Rothe M, Ko Y, Albers P, Wernert N. Eukaryotic initiation factor 3 p110 mRNA is overexpressed in testicular seminomas. *Am J Pathol* 2000; **157**: 1597–604.
- 45 Song N, Wang Y, Gu X, Chen Z, Shi L. Effect of siRNA-mediated knock-down of eIF3c gene on survival of colon cancer cells. *J Zhejiang Univ Sci B* 2013; **14**: 451–9.
- 46 Emmanuel R, Weinstein S, Landesman-Milo D, Peer D. eIF3c: a potential therapeutic target for cancer. *Cancer Lett* 2013; **336**: 158–66.
- 47 Asashima M, Ariizumi T, Malacinski GM. In vitro control of organogenesis and body patterning by activin during early amphibian development. *Comp Biochem Physiol B Biochem Mol Biol* 2000; **126**: 169–78.

## Supporting Information

Additional Supporting Information may be found online in the supporting information tab for this article:

**Table S1.** Primers of quantitative real-time PCR used in the study.

**Table S2.** siRNA sequence of *eIF3c*.

**Table S3.** Differentially expressed RNA-binding protein genes.

**Table S4.** *P*-values and hazard ratios of survival-associated RNA-binding protein genes.

**Table S5.** Differentially expressed genes induced by overexpression of *eIF3c*.

**Table S6.** Results of Gene Set Enrichment Analysis based on Kyoto Encyclopedia of Genes and Genomes pathways gene sets.

**Table S7.** Results of Gene Set Enrichment Analysis based on hallmark gene sets.

**Table S8.** Upregulated genes enriched in KRAS, VEGF, and Hedgehog signaling pathways for validation.

**Fig. S1.** Gene Ontology analysis of differentially expressed RNA-binding proteins (92 upregulated and 19 downregulated genes).

**Fig. S2.** Knockdown efficiencies of *eIF3c* measured by quantitative PCR and immunoblotting SMMC-7721 and SK-HEP-1 cells.

**Fig. S3.** Overexpressed efficiencies of *eIF3c* measured by quantitative PCR and immunoblotting SMMC-7721 and Huh-7 cells.